Journal of Applied Polymer Science

Curing kinetics of a "green" thiol-containing resin: Oligo(ethylene-2-mercaptosuccinate)

Michael Davis,[1] John P. Droske,[2] Wei Zheng[1]
[1]Department of Engineering and Technology, University of Wisconsin-Stout, Menomonie, Wisconsin 54751
[2]Department of Chemistry, University of Wisconsin-Stevens Point, Stevens Point, Wisconsin 54481
Correspondence to: W. Zheng (E-mail: zhengw@uwstout.edu)

ABSTRACT: This work focuses on examining the curing process of neat oligo(ethylene-2-mercaptosuccinate) using differential scanning calorimetry (DSC), rheology, and Fourier transform infrared (FTIR) spectroscopy. The thiol-containing resin offers much promise as a bioabsorbable polymer in medical field and as a reusable thermoset in sustainable applications. Although curing between thiol groups has been investigated in solutions, studies of neat materials without solvent are rare. Here, the evolution of glass transition temperature (T_g), complex shear modulus (G*), gelation, and chemical structure are monitored as a function of isothermal curing time and temperature. Both T_g and G^* increase with curing, indicating the formation of polymer networks. The conversion of the cure is determined from the DiBenedetto equation and is found to follow a second-order plus second-order autocatalytic reaction model. Importantly, the intensity of the S–H bond absorption decreases with the extent of curing, which confirms the curing mechanism, i.e., disulfide formation between the thiol groups. © 2015 Wiley Periodicals, Inc. J. Appl. Polym. Sci. **2016**, *133*, 43205.

KEYWORDS: crosslinking; differential scanning calorimetry (DSC); kinetics; rheology; thermosets

Received 13 August 2015; accepted 10 November 2015
DOI: 10.1002/app.43205

INTRODUCTION

Thiol-containing polymers have received much attention in recent years due to their promising medical applications and use in sustainable technologies. Good examples are stimulus-responsive hydrogels,[1–5] hosts for ions,[6] polymer encapsulation,[7,8] self-healing materials,[9,10] intra-ocular lenses,[11] and molecularly imprinted dendrimers.[12] In an effort to further understand and design such polymers, a "green" thermosetting resin, oligo(ethylene-2-mercaptosuccinate), has been prepared under solventless, zinc chloride catalyzed esterification conditions.[13,14] This oligomer contains thiol pendant groups which offer the possibility of reversible crosslinking in addition to ready degradation of the polymer main chain.[1–12] The monomers used in the synthesis can be obtained from non-petroleum renewable resources. For instance, one of the monomers, ethylene glycol, can be sourced from cellulosic biomass in a one-pot conversion.[15] Due to the non-nucleophilicity of the pendant thiols, it is expected that, upon curing, chemical linkages form between pendant thiol groups on the oligomers, and the crosslinking can be reversed by using appropriate reducing reagents, such as dithiothreitol. The ready hydrolysis of aliphatic ester linkages coupled with the reversible crosslinking offers potentials for applications in biomedical and others fields where recyclable and reusable "green" materials are desired. Particularly, the resin could compete with the leading biodegradable polymer, polylactic acid, which takes 40% of the current biodegradable plastics market.

To advance our knowledge of the resin and to provide guidance for processing, additional elucidation of the curing process is needed. As mentioned above, the majority of thiol crosslinking studies,[1–14] have focused on the synthesis and properties of fully cured samples particularly regarding mechanical, optical, and swelling responses. In several cases, the kinetics of curing has been examined but is primarily on solution kinetics in the presence of solvent. Jayaraman and coworkers[12] have studied the crosslinking of thiols and the disassembly of resultant disulfide crosslinks in poly(alkyl aryl ether) dendrimers by monitoring the sample's optical properties in solutions as a function of time. The authors find that the dendrimer cures faster at higher dendrimer concentrations and reversing the crosslinking is quicker with more concentrated dithiothreitol, a reagent known to cleave disulfide linkages. Lewis and coworkers[1] have determined the kinetics of de-crosslinking of disulfide-based triblock copolymers by examining the viscosity of the aqueous copolymer solution with the reducing agent of glutathione. Consistently, higher de-crosslinking rate is observed at higher

glutathione/disulfide molar ratios. In addition to the concentration dependence, de-crosslinking has also been found to strongly depend on the pH of the solution[11,16,17] and the force applied to the sulfide bond[18]. Ravi and coworkers[11] have compared the oxidation of aqueous solutions of thiol-containing copolyacrylamides in air under neutral conditions and with 3,3-dithiodipropionic acid. The exchange reaction under the acidic conditions yields a much faster curing rate. Although the curing between free thiol groups and its de-crosslinking event have been investigated in solutions, to the best of our knowledge, studies under thermal conditions only are rare. However, such studies are highly desirable for understanding the curing mechanism and for the target applications in the absence of solvent, i.e. the use of oligo(ethylene-2-mercaptosuccinate) as a sustainable thermoset. The lack of these studies further motivates the current work.

This work focuses on examining the curing process of neat oligo(ethylene-2-mercaptosuccinate). Due to the known slow reaction rate between free thiols,[19] the curing is conducted at elevated temperatures ranging from 170 to 220°C. The evolution of glass transition temperature (T_g) is followed using differential scanning calorimetry (DSC). The T_g data generated is used to determine the conversion of thiol groups and the curing kinetics. Based on this, we adopt a second-order and second-order autocatalytic reaction model to describe the curing. Additionally, in order to evaluate the mechanical integrity of the cured network, complex shear modulus and gelation are monitored during isothermal curing using rheological measurements. Structural changes in the material are recorded by Fourier transform infrared spectroscopy (FTIR) to establish the curing mechanism. The results obtained are discussed and compared with those found for thiol-containing systems in solutions and for polylactic acids.

EXPERIMENTAL

Materials

The resin used in this study is oligo(ethylene-2-mercaptosuccinate). The synthesis of the material has been reported previously[13] and is briefly summarized here (see Figure 1(a)). To a round bottom flask equipped with a condenser and with magnetic stirring, was added 7.54 g (0.0502 mol) of mercaptosuccinic acid, 15.7 mL (0.150 mol) of ethylene glycol, and 0.1742 g (0.00128 mol) of zinc chloride. The flask was flushed with nitrogen and then maintained under a static nitrogen atmosphere. The reaction mixture was heated at 150°C/h to 155°C and then maintained at 155°C for 4 h. After cooling to room temperature, 100 mL of methylene chloride was added to dissolve the product. The solution was washed twice with 100 mL of distilled water and twice with 100 mL of 50% saturated NaCl. The organic layer was dried over sodium sulfate, and the solvent was removed via rotary evaporation. Residual solvent was removed under reduced pressure (less than 1 mm Hg) at slightly above ambient temperature, and the structure was confirmed by FTIR, proton nuclear magnetic resonance (^{1}HNMR), and carbon-13 nuclear magnetic resonance (^{13}CNMR) spectroscopy. The number average molecular weight of the resin determined from gel permeation chromatography is ~2500 g/mol, with a polydispersity index around 1.7. The resin can be cured to highly transparent films and the proposed curing reaction is shown in Figure 1(b). The material was stored in a laboratory freezer maintained at −20°C before use.

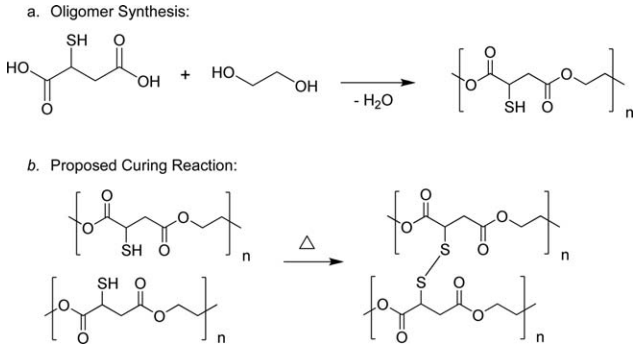

Figure 1. (a) Synthesis of oligo(ethylene-2-mercaptosuccinate) and (b) proposed curing reaction.

DSC Measurements

A differential scanning calorimeter from TA Instruments (TA Q20) was used for the calorimetric measurements. All the DSC runs were made under a nitrogen atmosphere. T_{zero} aluminum pans and hermetic lids were used. Sample sizes ranged from 10 to 22 mg. Isothermal curing was conducted at temperatures of 180, 200, and 220°C with curing times ranging from 0 to 5100 min. (Note that the curing temperatures chosen are much lower than the onset degradation temperature of the resin obtained from thermogravimetric measurements, 307°C, and therefore, significant thermal degradation is not expected during the curing process.) After curing for specific time, the samples were cooled at 20 K/min to −30°C and then reheated at 20 K/min to the desired curing temperature. The cycle was repeated until the curing was completed at this temperature. In order to examine whether the heating/cooling scans have effects on the curing results, results from short curing intervals, such as 10 min, are compared with those obtained with interval of 30 min or longer. The heating scans were used to monitor the evolution of the glass transition, as described below.

Glass transition temperature, T_g, is theoretically defined as the temperature on cooling where the heat capacity change of the system is half of the total change in the transition. In this work, the limited fictive temperature (T_f') was calculated from DSC heating scans. Since the T_f' measured on heating is found to be a good estimate of T_g at the same cooling rate (within 1 K),[20] T_f' is reported as the T_g throughout the text. We find T_f' by integrating the heat flow curve and then extrapolating the liquid line to the glassy line, a procedure consistent with the method proposed by Moynihan *et al.*[21]

$$\int_{T_f'}^{T\gg T_g}\left(C_{pl}-C_{pg}\right)dT=\int_{T\ll T_g}^{T\gg T_g}\left(C_p-C_{pg}\right)dT \qquad (1)$$

where C_{pl} and C_{pg} are the constant pressure heat capacities for the liquid and the glass, respectively, and C_p is the apparent heat capacity measured by DSC.

Temperature and heat flow calibrations of the DSC were performed on heating at 20 K/min with tin, indium, and gallium.

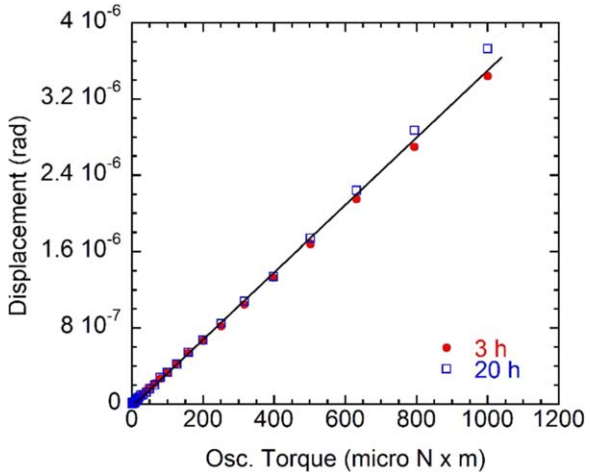

Figure 2. The displacement measured as a function of the torque for an 8 mm diameter platen. The results are obtained after the cure of an epoxy glue for 3 and 20 h at room temperature, respectively. [Color figure can be viewed in the online issue, which is available at wileyonlinelibrary.com.]

The three materials showed clear melting temperatures at 231.9, 156.6, and 29.8°C, respectively. Differences between the known values and those obtained were used to calibrate temperature readings on the TAQ20. The heat of fusion of indium, $\Delta H = 28.45$ J/g, was used to calibrate the heat flow. The temperature and heat flow were calibrated within ± 0.20 K and ± 0.2 J/g, respectively. The calibrations were checked at regular intervals by performing check runs using the three calibration standards.

Rheology

Frequency sweep measurements were performed to study the viscoelastic behavior using a rheometer from TA Instruments (TA AR2000ex). Disk-shaped samples of 8 mm diameter and 0.9 – 1.3 mm thickness were used for parallel plate rheometry. The sample was made directly inside the rheometer by loading the sample at 60°C, then gradually moving the upper plate up and down to form the disk-like sample. Nitrogen gas was used during the tests to minimize sample degradation. Measurements were conducted at 200°C with testing frequencies ranging from 0.3 to 30 rad/s. The strain amplitude used was less than 1%, within the linear viscoelastic region. In addition to the frequency sweep tests, time sweep measurements were conducted at different temperatures (170, 185, 200, and 210°C) to determine the gel point, i.e., the time to gelation.

One important issue in the experimental rheology field is the instrument compliance problem. As demonstrated by McKenna and coworkers,[22,23] without properly correcting the instrument compliance, errors would occur not only in the absolute values but also in the shape of the relaxation curve. In this work, the instrument compliance was first measured following the reported methodology.[22] As shown in Figure 2, where the deflection angle is plotted as a function of the applied torque, the instrument compliance determined from the slope was found to be 3.48×10^{-3} Nm/m. The value was input to the TA software, and the instrument compliance was corrected for all of the data shown. Additionally, the instrument inertia, geometry inertia, bearing friction, and thermal coefficient were calibrated for the rheometer. The quality of the calibrations was checked by running steady state viscosity measurements on a Cannon certified viscosity standard. For all runs, the average viscosities were within 2% of the values provided by the manufacturer, affirming that the rheometer calibrations were reliable and reproducible.

FTIR Measurements

Infrared spectroscopy experiments were performed using a Nicolet IS5 spectrometer, equipped with a single bounce attenuated total reflection (ATR) accessory. Samples cured in the DSC at 200°C for various times (0, 1, 3, 5, 8, 12, and 30 h) were used. All data were collected in the ATR mode at room temperature, with 8 cm^{-1} spectral resolution and averaging of 64 interferometric scans. Peak areas were calculated using the OMNIC software installed on the Nicolet IS5 instrument.

RESULTS AND DISCUSSION

The DSC heating scans are plotted in Figure 3 for the oligo(ethylene-2-mercaptosuccinate) after cured at 200°C for various times. The uncured sample shows a glass transition temperature (T_g) of approximately 2°C. As expected, with curing, T_g shifts to higher temperatures, and the breadth of the transition becomes broader particularly at intermediate curing times, such as 300 min. The broadening in the T_g might arise from a broader molecular weight distribution due to the presence of both long-chain polymer networks and short-chain oligomers.[24,25] From the heat flow curves, the T_g, and the heat capacity change at T_g (dC_p) are determined and shown in Figure 4 as the open symbols. For comparison, the data obtained at the same temperature but with constant 10 min curing interval are also plotted with solid symbols. The two sets of data seem to fall upon each other, indicating that the effects of the cooling and heating scans involved in the DSC measurements can be neglected on the extent of curing, consistent with the work of Simon and coworkers.[26] The T_g increases as the oligomers react with each other, and reaches 81.9 ± 0.7°C after being fully cured. The associated dC_p (shown in the inset of Figure 4) decreases

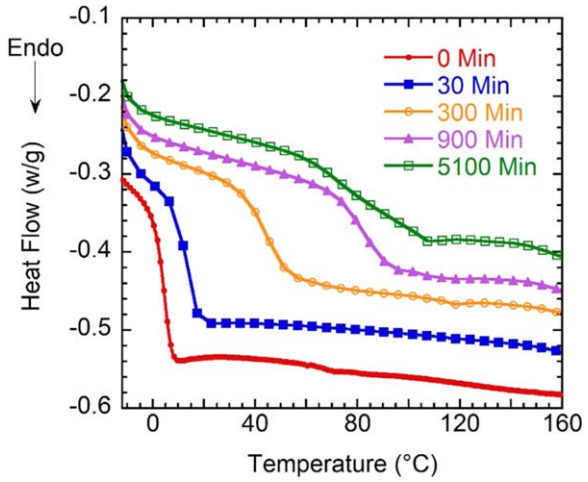

Figure 3. The representative DSC heat flow obtained on heating at 20 K/min after cooling at 20 K/min for oligo(ethylene)-2-mercaptosuccinate cured at 200°C for various times (0, 30, 300, 900, and 5100 min). [Color figure can be viewed in the online issue, which is available at wileyonlinelibrary.com.]

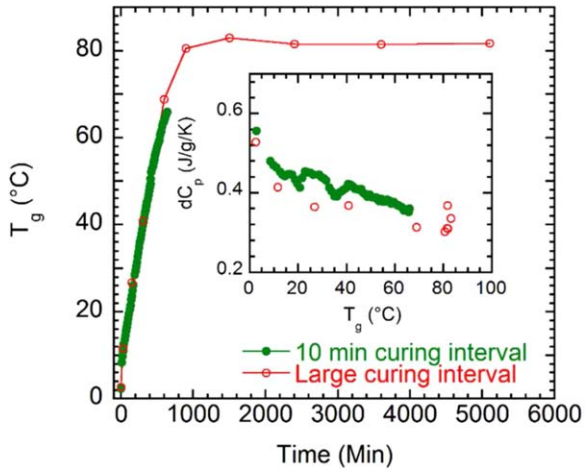

Figure 4. The glass transition temperature, T_g, plotted as a function of curing time at 200°C. The heat capacity change at T_g, dC_p, is plotted as the inset. Data obtained with short (10 min) and long (30 to 1500 min) curing interval are shown as solid and open symbols, respectively. Lines are given as visual guides. [Color figure can be viewed in the online issue, which is available at wileyonlinelibrary.com.]

from 0.569 ± 0.03 to 0.331 ± 0.03 J/g/K as the extent of curing increases. The reduced dC_p agrees with theoretical[27,28] and experimental[29] results that polymerization suppresses the rotational and translational contributions to the heat capacity, particularly to the liquid C_p.

In order to examine the effects of temperature on the curing process, the evolution of T_g and dC_p at other curing temperatures of 180 and 220°C are monitored and illustrated in Figures 5 and 6, along with those obtained at 200°C. Apparently, the resin cures faster at higher curing temperatures. The time required to complete the curing decreases from 42 h at 180°C to 25 h at 200°C and 17 h at 220°C. T_g of the fully cured materials is relatively the same, with an average of 82.0 ± 0.7°C (Note T_g of uncured sample is 2.0 ± 0.7°C). The associated dC_p (Figure 6) drops linearly with T_g, from 0.547 ± 0.02 to

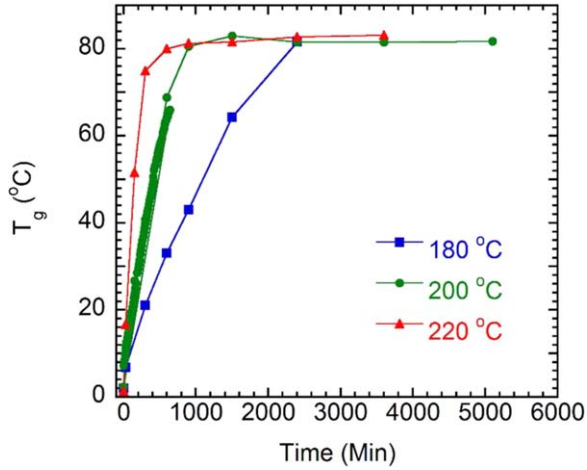

Figure 5. The glass transition temperature, T_g, plotted as a function of time during isothermal curing at 180, 200, and 220°C. Lines are given as guides to the eye. [Color figure can be viewed in the online issue, which is available at wileyonlinelibrary.com.]

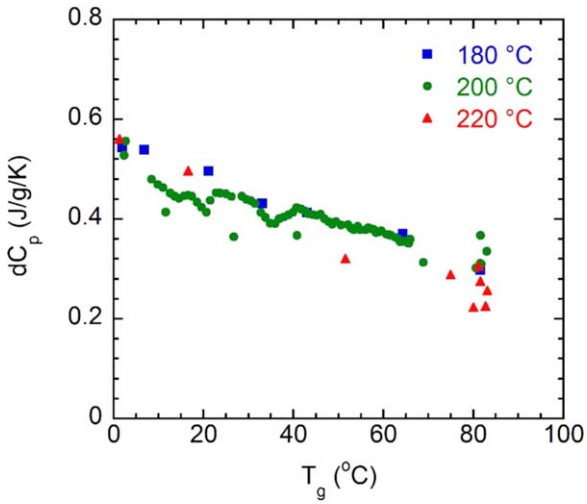

Figure 6. The associated heat capacity change at T_g, dC_p, is plotted as a function of T_g during isothermal curing at 180, 200, and 220°C. [Color figure can be viewed in the online issue, which is available at wileyonlinelibrary.com.]

0.272 ± 0.04 J/g/K for the uncured and fully cured samples, respectively. Such a linear relation is consistent with results on diepoxy-tetrafunctional diamine at different conversions.[30] The similar final T_g and relation with dC_p imply the possibility of using various curing routes to achieve desired material properties. As a potential resin to partially replace the leading biodegradable polymer on the market, polylactic acid, T_g of the fully cured oligo(ethylene-2-mercaptosuccinate) is 23 K higher than that found for polylactic acid.[31] The higher T_g of the cured resin would impart a wider use temperature window to the resin than has been observed with polylactic acids.

To further understand the curing process, the conversion of the curing is determined from the T_g and dC_p data using the DiBenedetto equation,[32] given by the following:

$$\frac{T_g - T_{g0}}{T_g^{\infty} - T_{g0}} = \frac{\lambda x}{1-(1-\lambda)x} \tag{2}$$

where T_{g0} represents the T_g of the uncured oligomer, T_g^{∞} is the maximum T_g obtained experimentally for the "fully cured" material, and λ is a structure-dependent material parameter.[33] The value of λ has been related to the step changes in the heat capacity for uncured and fully cured resins, ΔC_{p0} and ΔC_p^{∞}, respectively[33–38]:

$$\lambda = \frac{\Delta C_p^{\infty}}{\Delta C_{p0}} \tag{3}$$

(Note that, generally, conversion can also be determined from the heat of curing;[35] however, in this work, the heat dissipated from the curing is too subtle to be captured.) Based on the dC_p data shown in Figure 6, a λ of 0.497 ± 0.07 was calculated from eq. (3). With the λ, T_g, T_{g0}, and T_g^{∞}, the conversion of the curing is determined and plotted in Figure 7. To study the kinetics of curing, the conversion is fitted using a second-order plus second-order autocatalytic (third-order overall) equation[33]:

$$\frac{dx}{dt} = k(1-x)^2(x+b) \tag{4}$$

where x is conversion, t is cure time, k is the reaction rate constant, and b the ratio of the rate constants for the second-order

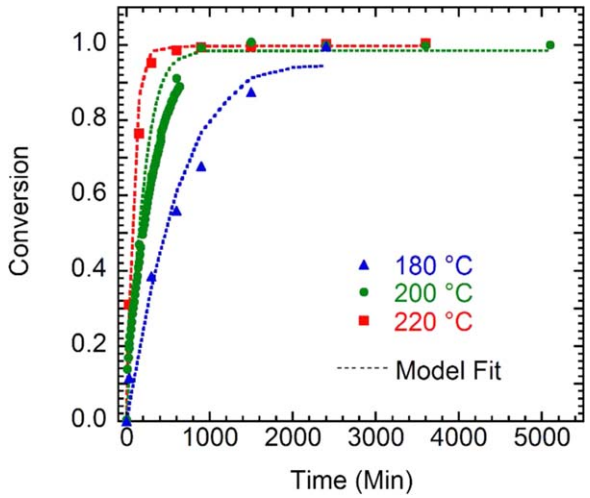

Figure 7. The conversion plotted a function of time for the isothermal curing conducted at 180, 200, and 220°C. Dashed line represents the best fit from the kinetic eq. (4). Standard deviations of the fit are 0.06, 0.09, and 0.04 for the data obtained at 180, 200, and 220°C, respectively. [Color figure can be viewed in the online issue, which is available at wileyonlinelibrary.com.]

and the second-order autocatalytic reactions. We would like to point out that although thiol-disulfide interchange reaction is proposed to be overall second order,[39] in this study, a second-order model tends to underpredict the T_g of fully cured samples and is not able to fit the entire range of the data. Instead, the third-order autocatalytic model describes the data well, shown as the dashed lines in Figure 7. The k obtained from the best fits of the model is plotted in Figure 8 as a function of curing temperature. The activation energy determined is 81.5 ± 2.5 kJ/mol, which is higher than thiol-disulfide exchange reaction observed in solutions, 9.4 – 66.2 kJ/mol.[40–42]

In addition to the evolution of T_g, the progression of mechanical properties during curing is also monitored. As shown in Figure 9, the complex shear modulus, G^*, obtained from curing at 200°C is plotted as a function of curing time. Uncured sample

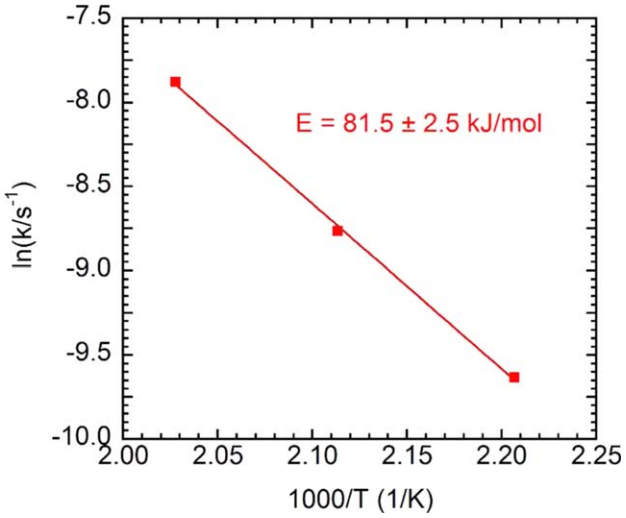

Figure 8. The curing rate constant k plotted a function of temperature, T. [Color figure can be viewed in the online issue, which is available at wileyonlinelibrary.com.]

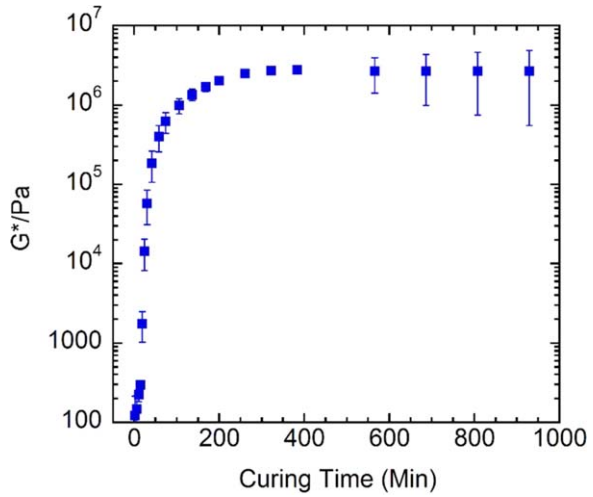

Figure 9. The complex shear modulus, G^*, is plotted as a function of curing time for oligo(ethylene)-2-mercaptosuccinate cured at 200°C. [Color figure can be viewed in the online issue, which is available at wileyonlinelibrary.com.]

shows a low modulus of 300 Pa (G_0^*). With curing, the modulus increases and gradually reaches 3.0 × 10^6 Pa ($G^{*\infty}$), much higher than that of polylactic acid, ~1.1 × 10^3 Pa, measured at the same temperature.[43] The increase in the complex shear modulus indicates the formation of polymer network with curing. The modulus seems to level off after curing for 400 min, slightly earlier than observed for T_g in the calorimetric measurements. This is not surprising since rheology and DSC might weight chain relaxation time differently.[20,24] If we adopt a similar model as eq. (2) but with G_0^* and $G^{*\infty}$ as T_{g0} and T_g^∞, and assume the same structure parameter λ, it is found that the conversion determined from G^* is compatible with that from the calorimetric T_g at conversion lower than 50% but is higher when the conversion rises above 50%. The results might indicate that, compared to the G^*, the calorimetric T_g is more sensitive to the unreacted pendant thiol groups. Although the reason behind this is unclear, the results are similar to what we found for polymer/oligomer blends[24] where obvious concentration effects are observed in the broadening of the calorimetric T_g but the rheological segmental region remains unchanged with blending.

Another important parameter regarding the curing process is the gelation point, which indicates the incipient formation of an infinite polymer network.[44] The commonly used criteria to determine the gel time include the time at which the loss tangent tanδ becomes independent of frequency,[45] the storage and loss moduli (G' and G'') cross each other,[46,47] and the viscosity of the resin approaches infinity.[48] Winter and Chambon[45] points out that the G'–G'' crossover only applies to a group of polymers in which the shear modulus G follows a power law relaxation with time t and with an exponent of 1/2, i.e., $G \sim t^{1/2}$. Examples of such polymers include stoichiometrically balanced systems and those with excess cross-linkers. For the general case, including imbalanced systems, the author recommends using the point at which the tanδ becomes frequency independent. Although the curing system of this work is expected to be

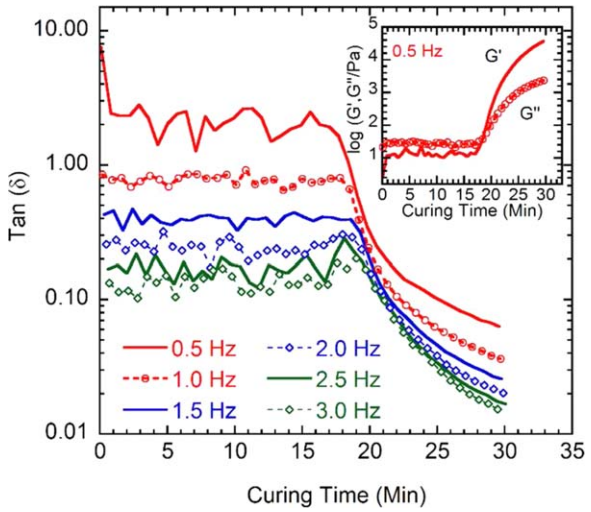

Figure 10. Storage, loss shear moduli (G' and G''), and the loss tangent, tanδ are plotted as a function of curing time for oligo(ethylene)-2-mercaptosuccinate cured at 210°C. Note that the data are scattered slightly due to the low modulus at the beginning of curing and the instrument resolution. [Color figure can be viewed in the online issue, which is available at wileyonlinelibrary.com.]

stoichiometrically balanced, the gelation time is determined using both criteria. As shown in Figure 10 for the isothermal curing at 210°C, the tanδ becomes frequency independent at 20 min, comparable to the time observed from the G'–G'' crossover, 17.9 min (see inset). Similar results are obtained for curing conducted at other temperatures, and the data are plotted in Figure 11. The gelation times measured with both criteria are consistent with each other, increasing from 18.9 ± 1.5 min at 210°C to 126.1 ± 4.6 min at 170°C. The temperature dependence of the gelation is further discussed next.

Assuming an Arrhenius temperature dependence of the reaction rate, the kinetics of curing can be expressed in the following form:

$$\frac{dx}{dt} = k_0 e^{-\frac{E}{RT}} g(x) \tag{5}$$

where x is the conversion, t is the curing time, k_0 is the pre-exponential frequency factor for the overall reaction, E is the apparent activation energy for the overall reaction, and $g(x)$ can be $(1\text{-}x)^2(x+b)$ as shown in eq. (4) or any unknown function of x and is assumed to be temperature independent. By integrating eq. (5) from zero to the gel time, t_{gel}, the relation between t_{gel} and reaction rate can be written as:

$$t_{gel} = \frac{1}{k_0 e^{-\frac{E}{RT}}} \int_0^{x_{gel}} \frac{1}{g(x)} dx. \tag{6}$$

Taking the natural logarithm on both sides yields:

$$\ln\ t_{gel} = ln\left[\frac{1}{k_0}\int_0^{x_{gel}} \frac{1}{g(x)} dx\right] + \frac{E}{RT}. \tag{7}$$

According to Flory,[49] the degree of cure at the gel point, x_{gel}, only depends on the functionality of the resin and is independent of the curing temperature. Therefore, the first term on the right side of eq. (7) can be assumed to be constant, c, and the equation reduces to

$$ln\ t_{gel} = c + \frac{E}{RT}. \tag{8}$$

By plotting $ln\ (t_{gel})$ vs. $1/T$ (Figure 11), the activation energy of gelation is determined to be 80.1 ± 6.3 kJ/mol. The value obtained is slightly higher than those reported for other thiol curing systems, 27.6 to 58.5 kJ/mol.[16,17,42]

Finally, in order to examine the curing mechanism, FTIR spectroscopy data are collected for the oligomer and the resin cured at 200°C for times up to 30 h. The representative absorption curves are shown in Figure 12. The peak at 2950 cm^{-1} represents the C–H stretching absorption; the peak at 2510 cm^{-1} is for the S–H thiol bond, and the peak at 1720 cm^{-1} is associated with the C=O in the carboxyl group.[50] During the cure, the intensity of the S–H peak decreases with the time of curing whereas the intensity of the C–H and C=O remains relatively constant. Note that, although the height of the C=O absorption peak decreases upon curing, the area under the peak is only about 3% lower. In this work, we use the intensity of C–H absorption peak as an internal standard considering its relatively similar intensity as the S–H peak of interest. The conversion of curing is determined based on the area change of the S–H absorbance peak, and the results are plotted in Figure 13, along with those calculated earlier from the DSC measurements. The two groups of data agree well, and the best fit of eq. (4) to the FTIR data yields similar curing rate constant as expected (0.000148 and 0.000156 1/s for FTIR and DSC, respectively). The results indicate that the curing likely proceeds through reaction between the thiol groups forming disulfide bonds. Due to its low polarity, the disulfide bond absorption is reported to be weak in the FTIR absorbance spectra, ~450 to 550 cm^{-1}.[51] The intensity of the disulfide absorption seems to increase with curing, but this cannot be confirmed with FTIR alone.

It is proposed that curing occurs by thermal reaction of the thiol groups to form disulfide linkages. The thiol groups clearly

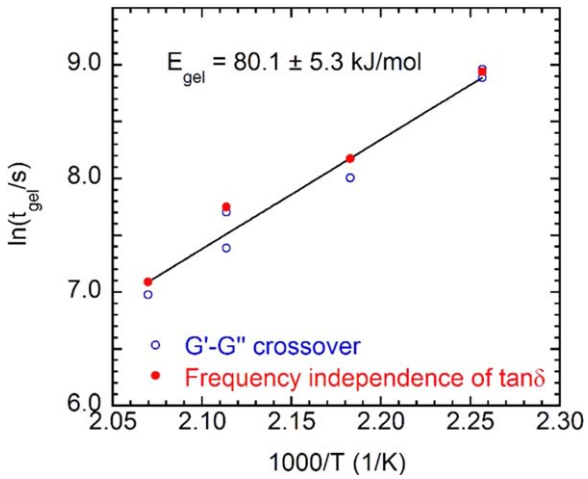

Figure 11. Gel time, t_{gel}, as a function of the isothermal curing temperature, T. [Color figure can be viewed in the online issue, which is available at wileyonlinelibrary.com.]

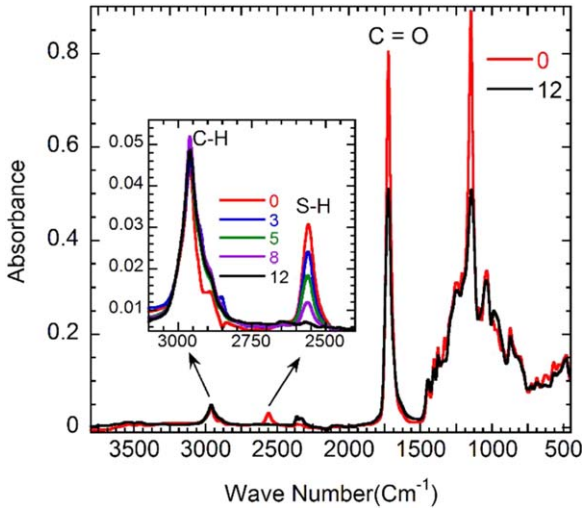

Figure 12. FTIR spectra of the uncured and cured oligo(ethylene)-2-mercaptosuccinate at 200°C for different times (3, 5, 8, and 12 h). The inset shows the enlarged peaks for C–H and S–H absorption. [Color figure can be viewed in the online issue, which is available at wileyonlinelibrary.com.]

are involved in the curing reaction as evidenced by the decrease in the intensity of the thiol absorption during curing as shown by FTIR. In addition, consistent conversions were noted between the calorimetric and FTIR data. Furthermore, the observed conversion at gel point, x_{gel}, agrees with the theoretically predicted value based on the proposed thiol group reaction. The measured gelation time at 200°C is 36 min, which corresponds to a conversion of 0.22 (Figure 7). From the statistical approaches developed by Flory[49,52] or Macosko and coworkers,[53] x_{gel} can be calculated from,

$$x_{gel} = \frac{1}{[r(f-1)]^{0.5}}$$

where r is the stoichiometric ratio of reactional groups and f represents the functionality of the oligomer. In this study, $r = 1$ and $f = 24$, the number of repeating unit of the oligomer. The

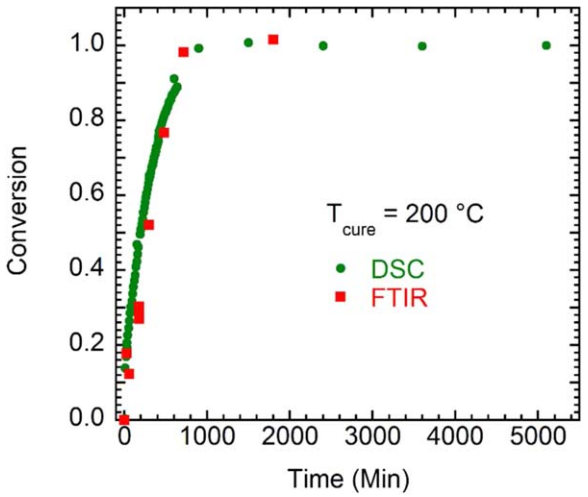

Figure 13. Conversions determined from FTIR and DSC measurements for oligo(ethylene)-2-mercaptosuccinate samples cured at 200°C for various times ranging from 0 to 5100 min. [Color figure can be viewed in the online issue, which is available at wileyonlinelibrary.com.]

conversion at gelation is determined to be 0.21, in excellent agreement with experimentally obtained value. The calorimetric and rheological measurements were performed under a nitrogen atmosphere, which should exclude possible reactions with oxygen. Importantly, the thiol groups are non-nucleophilic under the synthesis and curing conditions and no thioester formation has been observed by FTIR. This material clearly shows potential as a sustainable thermoset that exhibits the desirable features of crosslinked materials coupled with the hydrolytic properties of aliphatic polyesters.

CONCLUSIONS

The curing process of a "green" thiol-containing resin, oligo(ethyylene-2-mercaptosuccinate), has been investigated using differential scanning calorimetry, rheology, and Fourier transform infrared spectroscopy. The evolution of T_g and dC_p are monitored during isothermal curing at 180, 200, and 220°C, respectively. As expected, the resin cures faster at higher curing temperatures. The time required to complete the curing decreases from 42 h at 180°C to 25 h at 200°C and 17 h at 220°C. On average, T_g increases from 1.97 ± 0.7 to 82.0 ± 0.7°C, along with dC_p decreasing from 0.547 ± 0.02 to 0.272 ± 0.04 J/g/K. A linear relation is found between the dC_p and T_g, consistent with literature findings on other curing systems. The conversion is determined based on the DiBenedetto equation and is well fitted with a second-order and second-order autocatalytic reaction model. An activation energy of 81.5 ± 2.5 kJ/mol, which is higher that of curing occurred in solutions. Concurrent with the rise in T_g, the complex shear modulus increases to 6.5×10^6 Pa after being fully cured at 200°C. The gelation time is measured from the frequency independence of the loss tangent and from the crossover of G' and G''. Both yield similar results for the stoichiometrically balanced systems. In addition, it is found that the intensity of S–H bond absorption decreases with increasing curing time. The conversion determined from FTIR agrees with that from the calorimetric measurements, supporting a curing mechanism involving disulfide bond formation between thiol groups.

ACKNOWLEDGMENTS

We thank Garrett Sternhagen and Neiko Levenhagen at the University of Wisconsin-Stevens Point for synthesis of the resin. Financial support from the University of Wisconsin System and WiSys Technology Foundation through AR-WiTAG Match grant (106-SYS-06-8000-4) is also gratefully acknowledged.

REFERENCES

1. Li, C.; Madsen, J.; Armes, S. P.; Lewis, A. L. *Angew. Chem. Int. Ed.* **2006**, *45*, 3510.
2. Tsarevsky, N. V.; Matyjaszewski, K. *Macromolecules* **2002**, *35*, 9009.
3. Tsarevsky, N. V.; Matyjaszewski, K. *Macromolecules* **2005**, *38*, 3087.
4. Shu, X.; Liu, Y.; Luo, Y.; Roberts, M. C.; Prestwich, G. D. *Biomacromolecules* **2002**, *3*, 1304.

5. Chujo, Y.; Sada, K.; Naka, A.; Nomura, R.; Saegusa, T. *Macromolecules* **1993**, *26*, 883.
6. Corbett, P. T.; Tong, L. H.; Sanders, J. K. M.; Otto, S. *J. Am. Chem. Soc.* **2005**, *127*, 8902.
7. Zelikin, A. N.; Quinn, J. F.; Caruso, F. *Biomacromolecules* **2006**, *7*, 27.
8. Zelikin, A. N.; Li, Q.; Caruso, F. *Chem. Mater.* **2008**, *20*, 2655.
9. Bergman, S. D.; Wudl, F. *J. Mater. Chem.* **2008**, *18*, 41.
10. Pepels, M.; Filot, I.; Klumperman, B.; Goossens, H. *Polym. Chem.* **2013**, *4*, 4955.
11. Aliyar, H. A.; Hamilton, P. D.; Ravi, N. *Biomacromolecules* **2005**, *6*, 204.
12. Kiran, B. M.; Jayaraman, N. *Macromolecules* **2009**, *42*, 7353.
13. Juetten, M.; Kraft, G.; Huberty, W.; Pieper, R.; Droske, J. P. *Polym. Prints (ACS)* **2012**, *53*, 339.
14. Droske, J. P.; Juetten, M. J. U.S. Patent US2011/0269903 A1, **2011**.
15. Wang, A.; Zhang, T. *Acc. Chem. Res.* **2013**, *46*, 1377.
16. Chiou, B.; English, R. J.; Khan, S. A. *Macromolecules* **1996**, *29*, 5368.
17. Hoyle, C. E.; Hensel, R. D.; Grubb, M. B. *J. Polym. Sci. Polym. Chem. Ed.* **1984**, *22*, 1865.
18. Wiita, A. P.; Ainavarapu, S. R. K.; Huang, H. H.; Fernandez, J. M. *Proc Natl Acad Sci USA* **2006**, *103*, 7222.
19. Ghosh, K.; Shu, X. Z.; Mou, R.; Lombardi, J.; Prestwich, G. D.; Rafailovich, M. H.; Clark, R. A. F. *Biomacromolecules* **2005**, *6*, 2857.
20. Badrinarayanan, P.; Zheng, W.; Li, Q.; Simon, S. L. *J. Non-Cryst. Solids* **2007**, *353*, 2603.
21. Moynihan, C. J.; Easteal, A. J.; DeBolt, M. A.; Tucker, J. *J. Am. Ceram. Soc.* **1976**, *59*, 1216.
22. Schröter, K.; Hutcheson, S. A.; Shi, X.; Mandanici, A.; McKenna, G. B. *J. Chem. Phys.* **2006**, *125*, 214507.
23. Hutcheson, S. A.; McKenna, G. B. *J. Chem. Phys.* **2008**, *129*, 074502.
24. Zheng, W.; McKenna, G. B.; Simon, S. L. *Polymer* **2010**, *51*, 4899.
25. Zheng, W.; Simon, S. L. *J. Polym. Sci. Part B Polym. Phys.* **2008**, *46*, 418.
26. Koh, Y. P.; Simon, S. L. *J. Phys. Chem. B* **2010**, *114*, 7727.
27. Loufakis, K.; Wunderlich, B. *J. Phys. Chem.* **1998**, *92*, 4205.
28. Pyda, M.; Wunderlich, B. *Macromolecule* **1999**, *32*, 2044.
29. Huang, D.; Simon, S. L.; McKenna, G. B. *J. Chem. Phys.* **2005**, *122*, 084907.
30. Venditti, R. A.; Gillham, J. K. *J. Appl. Polym. Sci.* **1997**, *64*, 3.
31. Henricks, J.; Boyum, M.; Zheng, W. *J. Therm. Anal. Calorim.* **2015**, *120*, 1765.
32. Nielsen, L. E. *J. Macromol. Sci. Rev. Macromol. Chem.* **1969**, *C3*, 69.
33. Simon, S. L.; Gillham, J. K. *J. Appl. Polym. Sci.* **1993**, *47*, 461.
34. Pascault, J. P.; Williams, R. J. J. *J. Polym. Sci. Part B Polym. Phys.* **1990**, *28*, 85.
35. Li, Q.; Simon, S. L. *Macromolecules* **2009**, *42*, 3573.
36. Wisanrakkit, G.; Gillham, J. K. *J. Appl. Polym. Sci.* **1990**, *41*, 2885.
37. Simon, S. L.; Gillham, J. K. *J. Appl. Polym. Sci.* **1992**, *46*, 1245.
38. Hale, A.; Macosko, C. M.; Bair, H. E. *Macromolecules* **1991**, *24*, 2610.
39. Singh, R.; Whitesides, G. M. In The Chemistry of Sulphur-Containing Functional Groups; Patai, S., Rappoport, Z., Eds.; John Wiley & Sons: Chichester, West Sussex, England, **1993**; p 634.
40. Qi, P. X.; Nuñez, A.; Wickham, E. D. *J. Agric. Food Chem.* **2012**, *60*, 4327.
41. Fernandes, P. A.; Ramos, M. *J. Chem. Eur. J.* **2004**, *10*, 257.
42. Cook, W. D.; Chen, F.; Pattison, D. W.; Hopson, P.; Beaujon, M. *Polym. Int.* **2007**, *56*, 1572.
43. Henricks, J.; Davis, M.; Zheng, W. In Thermal and Rheological Characterization of Polylactic Acid, Proceedings of the 71st Annual Technical Conference of the Society of Plastics Engineers, Cincinnati, OH, April 22–24, **2013**.
44. Flory, P. In Selected Work of Paul J. Flory; Mandelkern, L., Ed., Stanford University Press: Redwood City: **1985**; p 136.
45. Winter, H. H.; Chambon, F. *J. Rheol.* **1986**, *30*, 367.
46. Tung, C. Y. M.; Dynes, P. J. *J. Appl. Polym. Sci.* **1982**, *27*, 569.
47. D4473 −08, Standard Test Method for Plastics: Dynamic Mechanical Properties: Cure Behavior, ASTM International, **2008**.
48. Mijovic, J.; Kenny, J. M.; Nicolais, L. *Polymer* **1993**, *34*, 207.
49. Flory, P. J. Principles of Polymer Chemistry; Cornell University Press: Ithaca: **1953**.
50. Naranjo, A.; Noriega, M. d. P.; Ossawald, T.; Roldan-Alzate, A.; Sierra, J. D. Plastics Testing and Characterization: Industrial Applications; Hanser: Cincinnati, **2008**; p 15.
51. Yan, B. Analytical Methods in Combinatorial Chemistry; Technomic Publishing Company: Lancaster, **2000**; p 58.
52. Odian, G. Principles of Polymerization; Wiley: New York, **1991**; p 103.
53. Miller, M. R.; Macosko, C. W. *Macromolecules* **1976**, *9*, 211.